Modeling of Optical Pulse Propagation in Kerr and Raman Nonlinear Dispersive Media Using JE-TLM Method

Abdellah Attalhaoui[1, *], Hamid Bezzout[2], El Hadi El Ouardy[2], Mouna Hanna[2],Mohamed Habibi[1], and Hanan El Faylali[2]

Abstract—In this paper, we propose a simulation model of electromagnetic wave's propagation in media with different kinds of dispersions. This model exploits the dependence of the polarization current density and the voltage electric in the context of the Transmission Line Matrix method with the Symmetrical Condensed Node (SCN-TLM) and novel voltage sources. By solving Maxwell's and polarization current density equations, the proposed model, named JE-TLM, gives a full solution of Maxwell's equations and polarization terms which describe the Lorentz linear dispersion, nonlinear instantaneous Kerr and retarded Raman effects. The scattering matrix characterizing the SCN with the new voltage sources is provided, and the numerical results are compared with those of the literature or with the theoretical ones.

1. INTRODUCTION

After the observation of second harmonic generation in 1961 [1], the study of nonlinear phenomena have been interesting research topics for both physicists and chemists. In general, the generation of light using laser sources with very high optical intensities through nonlinear optical media leads to the appearance of a number of nonlinear optical effects, and the most important ones are related to the third-order susceptibility $\chi^{(3)}$, including the Kerr effect and Raman effect [2].

On the one hand, the Kerr effect is a nonlinear optical effect resulting from instantaneous electronic response of such media to laser excitation. The interaction of electromagnetic waves with the media leads to modifying the refractive index which itself modifies the polarization of incident pulses.

On the other hand, the Raman effect is a nonlinear optical effect originated from the vibrations of the molecular of the medium to the laser excitation, which leads to the increase of temperature. This effect is named Raman scattering when these vibrations are associated with optical phonons. Both the effects, Raman and Kerr, are generated most of the time simultaneously. Numerous papers have been published, after the discovery of solitons in optical fibers in 1973 [3], which are related to the studies of nonlinearities that are exhibited by photonic crystal [4], microresonators [5], microfluidics [6], glass [7] and other media reported in [8]. In particular, in optical fiber technology, the Kerr and Raman nonlinearities present an active area of research with high interest. These nonlinearities can become strong effects and can be observed even at low power levels [1].

In nonlinear media, various time-domain numerical methods implementing different algorithms to solve the problems of the propagation of electromagnetic waves and their interaction with dispersive materials have already been proposed in literature. One of those methods is the finite-difference time-domain (FDTD) [9, 10], but Transmission Line Matrix is considered the most powerful and efficient method that gives a more precise results. This method was proposed by Johns [11], based on the

Principe of Huygens, and makes the analogy between the components of the electromagnetic field and circuit parameters. One of these algorithms that have been incorporated with the TLM method is the Z-transform technique [12], and another is CRC-TLM recursive convolution (CRC) combined to voltage and current sources [13] and the Auxiliary Differential Equation ADE-TLM [14]. However in our case, we use the JE-TLM that exploits the current density and the electric field that has been used to model isotropic cold plasma [15, 16] and used to simulate the propagation of optical pulses in two-level atomic systems [17]. In this paper, we increase a novel algorithm based on the JE-TLM method with condensed symmetrical node (SCN) and new voltage sources.

This approach allows implementation of optical pulse propagation in linear Lorentz and nonlinear Kerr and Raman media together. As the ADE-FDTD, the JE-TLM is more efficient to treat nonlinear effects because no assumption of the linearity of the medium is made [18].

The simulation results of our algorithm are compared with those of the literature or with the theoretical ones.

2. FORMULATIONS AND EQUATIONS

The Maxwell's equations for wave propagation in dispersive media using polarization current density are given by [19]

$$\nabla \times \mathbf{E} = -\mu_0 \frac{\partial \mathbf{H}}{\partial t} \tag{1}$$

$$\nabla \times \mathbf{H} = \varepsilon_0 \varepsilon_\infty \frac{\partial \mathbf{E}}{\partial t} + \mathbf{J} \tag{2}$$

where $\mathbf{E}$ and $\mathbf{H}$ are the electric and magnetic field vectors; μ_0 is the free space permeability; ε_0 is the free space permittivity; ε_∞ is the relative dielectric constant in the limit of infinite frequency and

$$\mathbf{J} = \frac{\partial \mathbf{P}}{\partial t} = \mathbf{J}_L + \mathbf{J}_{Kerr} + \mathbf{J}_{Raman} \tag{3}$$

is the polarization current density that is the sum of linear Lorentz polarization current, instantaneous Kerr nonlinear polarization current and Raman nonlinear polarization current.

2.1. Linear Lorentz Polarization Current

The relative permittivity of the Lorentz medium in the frequency domain can be expressed by [18]

$$\varepsilon(\omega) = \varepsilon_\infty + \frac{\Delta \varepsilon_L w_L^2}{w_L^2 + 2jw\delta_L - w^2} \tag{4}$$

where $\Delta \varepsilon_L = \varepsilon_s - \varepsilon_\infty$ is the change in relative permittivity, w_L the Lorentz characteristic resonant frequency, and δ_L the damping factor. A polarization current in the frequency domain is as follows

$$\widetilde{\mathbf{J}} = \Delta \varepsilon_L w_L^2 \varepsilon_0 \left(\frac{jw}{w_L^2 + 2jw\delta_L - w^2} \right) \widetilde{\mathbf{E}} \tag{5}$$

Multiplying both sides of Equation (5) by $(w_L^2 + +2jw\delta_L - w^2)$ and transforming to the time domain $jw \to \partial/\partial t$ and $w^2 \to -\partial^2/\partial t^2$ yields

$$w_L^2 \mathbf{J}_L + 2\delta_L \frac{\partial \mathbf{J}_L}{\partial t} + \frac{\partial^2 \mathbf{J}_L}{\partial t^2} = \Delta \varepsilon_L w_L^2 \varepsilon_0 \frac{\partial \mathbf{E}}{\partial t} \tag{6}$$

Applying the finite-difference-time to Equation (6), the linear polarization current density centered at $n + 1$ can be expressed as:

$$\mathbf{J}_L^{n+1} = \alpha_L \mathbf{J}_L^n + \xi_L \mathbf{J}_L^{n-1} + \gamma_L \frac{\mathbf{E}^{n+1} - \mathbf{E}^{n-1}}{2\Delta t} \tag{7}$$

where

$$\alpha_L = \frac{2 - w_L^2 (\Delta t)^2}{1 + \delta_L \Delta t}, \quad \xi_L = \frac{\delta_L \Delta t - 1}{1 + \delta_L \Delta t}, \quad \gamma_L = \frac{\varepsilon_0 \beta_L w_L^2 (\Delta t)^2}{1 + \delta_L \Delta t} \tag{8}$$

2.2. Nonlinear Kerr Polarization Current

The polarization is caused by the instantaneous Kerr nonlinearity as follows [19]:

$$\mathbf{P}_{Kerr}(t) = \varepsilon_0 \chi_0^{(3)} \mathbf{E} \int_{-\infty}^{t} \alpha \delta\left(t - t'\right) \mathbf{E}^2\left(t'\right) dt' = \alpha \varepsilon_0 \chi_0^{(3)} \mathbf{E}^3(t) \tag{9}$$

where $\chi_0^{(3)}$ denotes the nonlinear coefficient, and α parameterizes the relative strengths of the Kerr and Raman interactions. Applying the finite-difference-time to Equation (9), the nonlinear Kerr polarization current density centered at $n+1$ can be expressed as:

$$\mathbf{J}_{Kerr}^{n+1} = \frac{\alpha \varepsilon_0 \chi_0^{(3)}}{2\Delta t} \left\{ \left(|\mathbf{E}^{n+1}|\right)^2 \mathbf{E}^{n+1} - \left(|\mathbf{E}^{n-1}|\right)^2 \mathbf{E}^{n-1} \right\} \tag{10}$$

2.3. Nonlinear Raman Polarization Current

The polarization is caused by the Raman effect as follows [10]:

$$\mathbf{P}_{Raman}(t) = \varepsilon_0 \mathbf{E}(t) \int_{0}^{t} \chi_{Raman}^{(3)}\left(t - t'\right) * \mathbf{E}\left(t'\right) dt' = \varepsilon_0 \mathbf{E}(t) \left[\chi_{Raman}^{(3)}(t) * \mathbf{E}^2(t) \right] \tag{11}$$

To solve Equation (11), we need to introduce an auxiliary variable for the convolution

$$S(t) = \chi_{Raman}^{(3)}(t) * |\mathbf{E}(t)|^2 \tag{12}$$

Using the Fourier transform, Equation (12) becomes:

$$S(\omega) = \chi_{Raman}^{(3)}(\omega) \cdot \mathcal{F}|\mathbf{E}(t)|^2 \tag{13}$$

where

$$\chi_{Raman}^{(3)}(\omega) = \frac{(1 - \alpha)\chi_0^{(3)}\omega_{Raman}^2}{\omega_{Raman}^2 + 2j\omega\delta_{Raman} - \omega^2} \tag{14}$$

$$\omega_{Raman} = \sqrt{\frac{\tau_1^2 + \tau_2^2}{\tau_1^2 \tau_2^2}}, \quad \delta_{Raman} = \frac{1}{\tau_2} \tag{15}$$

By the use of Equation (14), Equation (13) can be rewritten as:

$$S(\omega) = \frac{(1 - \alpha)\chi_0^{(3)}\omega_{Raman}^2}{\omega_{Raman}^2 + 2j\omega\delta_{Raman} - \omega^2} \mathcal{F}|\mathbf{E}(t)|^2 \tag{16}$$

Multiplying Equation (16) by $\omega_{Raman}^2 + 2j\omega\delta_{Raman} - \omega^2$ followed by the inverse Fourier transformation leads to:

$$\omega_{Raman}^2 S + 2\delta_{Raman}\frac{\partial S}{\partial t} + \frac{\partial^2 S}{\partial t^2} = (1 - \alpha)\chi_0^{(3)}\omega_{Raman}^2 |\mathbf{E}|^2 \tag{17}$$

By discretizing Equation (17), the difference equation for S can be expressed as:

$$S^{n+1} = a_{Raman}S^n + b_{Raman}S^{n-1} + c_{Raman}(|\mathbf{E}^n|)^2 \tag{18}$$

with

$$a_{Raman} = \frac{2 - \omega_{Raman}^2(\Delta t)^2}{\delta_{Raman}\Delta t + 1} \tag{19}$$

$$b_{Raman} = \frac{\delta_{Raman}\Delta t - 1}{\delta_{Raman}\Delta t + 1} \tag{20}$$

$$c_{Raman} = \frac{(1 - \alpha)\chi_0^{(3)}\omega_{Raman}^2(\Delta t)^2}{\delta_{Raman}\Delta t + 1} \tag{21}$$

we can reformulate the expression of the polarization for the Raman effect described by Equation (11):

$$\mathbf{P}_{Raman}(t) = \varepsilon_0 \mathbf{E}(t) S(t) \tag{22}$$

By the use of Equation (22), the polarization current density of Raman is as follows:

$$\mathbf{J}_{Raman}(t) = \frac{\partial \mathbf{P}_{Raman}}{\partial t} = \frac{\partial}{\partial t} \varepsilon_0 \mathbf{E}(t) \ S(t) \tag{23}$$

Applying the finite-difference-time to Equation (23), the nonlinear Raman polarization current density centered at $n+1$ can be expressed as:

$$\mathbf{J}_{Raman}^{n+1} = \frac{\varepsilon_0}{2\Delta t} \left(\mathbf{E}^{n+1} S^{n+1} - \mathbf{E}^{n-1} S^{n-1} \right) \tag{24}$$

2.4. JE-TLM Approach

For the regular mesh, the TLM method makes the analogy between the electric field and voltage using this equation

$$\mathbf{E}^n = \frac{V^n}{\Delta l} \tag{25}$$

implementing Equation (25) into Equations (7), (10) and (24), the linear Lorentz polarization current, nonlinear Kerr polarizaton current and nonlinear Raman polarization current become respectively as follows:

$$\mathbf{J}_L^{n+1} = \alpha_L \mathbf{J}_L^n + \xi_L \mathbf{J}_L^{n-1} + \gamma_L \frac{V^{n+1} - V^{n-1}}{2\Delta t \Delta l} \tag{26}$$

$$\mathbf{J}_{Kerr}^{n+1} = \frac{\alpha \varepsilon_0 \chi_0^{(3)}}{2\Delta t \Delta l} \left\{ \left(|V^{n+1}| \right)^2 V^{n+1} - \left(|V^{n-1}| \right)^2 V^{n-1} \right\} \tag{27}$$

$$\mathbf{J}_{Raman}^{n+1} = \frac{\varepsilon_0}{2\Delta t \Delta l} \left(V^{n+1} S^{n+1} - V^{n-1} S^{n-1} \right) \tag{28}$$

Apply the model (SCN-TLM) to Equation (1) we obtain:

$$\begin{pmatrix} \nabla \times H_x^{n+\frac{1}{2}} \\ \nabla \times H_y^{n+\frac{1}{2}} \\ \nabla \times H_z^{n+\frac{1}{2}} \end{pmatrix} = \begin{pmatrix} \frac{\varepsilon_0}{2\Delta t \Delta l} \left[\left(V_1^i + V_2^i + V_9^i + V_{12}^i \right)^{n+1} - \left(V_1^r + V_2^r + V_9^r + V_{12}^r \right)^n \right] \\ \frac{\varepsilon_0}{2\Delta t \Delta l} \left[\left(V_3^i + V_4^i + V_8^i + V_{11}^i \right)^{n+1} - \left(V_3^r + V_4^r + V_8^r + V_{11}^r \right)^n \right] \\ \frac{\varepsilon_0}{2\Delta t \Delta l} \left[\left(V_5^i + V_6^i + V_7^i + V_{10}^i \right)^{n+1} - \left(V_5^r + V_6^r + V_7^r + V_{10}^r \right)^n \right] \end{pmatrix} \tag{29}$$

where

$$\left(V_1^r + V_2^r + V_9^r + V_{12}^r \right)^n = \left(V_1^i + V_2^i + V_9^i + V_{12}^i \right)^n + V_{sx}^{\ n} \tag{30}$$

$$\left(V_3^r + V_4^r + V_8^r + V_{11}^r \right)^n = \left(V_3^i + V_4^i + V_8^i + V_{11}^i \right)^n + V_{sy}^{\ n} \tag{31}$$

$$\left(V_5^r + V_6^r + V_7^r + V_{10}^r \right)^n = \left(V_5^i + V_6^i + V_7^i + V_{10}^i \right)^n + V_{sz}^{\ n} \tag{32}$$

By discretizing Equation (2), integrating Equations (30), (31), (32) and (29), making the analogy between the electric field and voltage by the use of Equation (25), and using the symmetrical condensed node (SCN-TLM), the total electric can be expressed as:

$$\begin{pmatrix} V_x^{n+1} \\ V_y^{n+1} \\ V_z^{n+1} \end{pmatrix} + \frac{A_2}{A1} \begin{pmatrix} |V_x^{n+1}|^2 \\ |V_y^{n+1}|^2 \\ |V_z^{n+1}|^2 \end{pmatrix} \begin{pmatrix} V_x^{n+1} \\ V_y^{n+1} \\ V_z^{n+1} \end{pmatrix} = \frac{2}{4 + \mathrm{Y}_{ox}} \begin{pmatrix} \left[V_1^i + V_2^i + V_9^i + V_{12}^i + 0.5\, V_{sx} \right]^{n+1} \\ \left[V_3^i + V_4^i + V_8^i + V_{11}^i + 0.5\, V_{sy} \right]^{n+1} \\ \left[V_5^i + V_6^i + V_7^i + V_{10}^i + 0.5\, V_{sz} \right]^{n+1} \end{pmatrix} \tag{33}$$

where

$$A_1 = \varepsilon_\infty + \frac{S^{n+1}}{2}, \quad A_2 = \frac{\alpha \chi_0^{(3)}}{2\Delta l^2} \tag{34}$$

The voltage sources (Vsx, Vsy, Vsz), by using the same procedure presented in [15, 20], can be expressed as:

$$
\begin{pmatrix} Vsx \\ Vsy \\ Vsz \end{pmatrix}^{n+1} = -\begin{pmatrix} Vsx \\ Vsy \\ Vsz \end{pmatrix}^{n} + 4\left[(\varepsilon_\infty - A_1)\begin{pmatrix} V_x^n \\ V_y^n \\ V_z^n \end{pmatrix} + 2A_2 \begin{pmatrix} V_x^{n3} \\ V_y^{n3} \\ V_z^{n3} \end{pmatrix} \right.
$$
$$
\left. -\frac{\Delta l \Delta t}{\varepsilon_0} \begin{pmatrix} J_{Lorentz,x} \\ J_{Lorentz,y} \\ J_{Lorentz,z} \end{pmatrix}^{n+1} + \frac{S^{n-1}}{2} \begin{pmatrix} V_x^{n-1} \\ V_y^{n-1} \\ V_z^{n-1} \end{pmatrix} \right] \tag{35}
$$

The normalized admittance at time $(n+1)\Delta t$ can be expressed as:

$$
_{n+1}Y_{ox} = \varepsilon_\infty + \frac{S^{n+1}}{2} - 1 \tag{36}
$$

The JE-TLM model with voltage sources is based on recursive calculation of normalized admittance made in Equation (36) and the voltage sources expressed in Equation (35). The obtained values are then inserted in Equation (33). The solution of the last equation is then used in the calculation of reflected pulses and in the connection process along the TLM mesh nodes. With this manner we can simulate the propagation of signal in each position and each time.

3. NUMERICAL RESULT

We now present the results of numerical tests to validate the formulations of Section 2. The air-nonlinear dispersive medium interface is located at $z = 8\Delta l$ with the spatial resolution $\Delta l = 10\,\text{nm}$. The network is divided into $(1, 1, 20000)\Delta l$. The excitation pulse is modulated with the hyperbolic secant function with a characteristic time constant 14.6 fs, initial maximum field intensity 1 V/m, and carrier frequency $f_c = 1.37 \times 10^{14}\,\text{Hz}$. For both cases, linear and nonlinear dispersions, we analyze by selecting the following parameters [10].
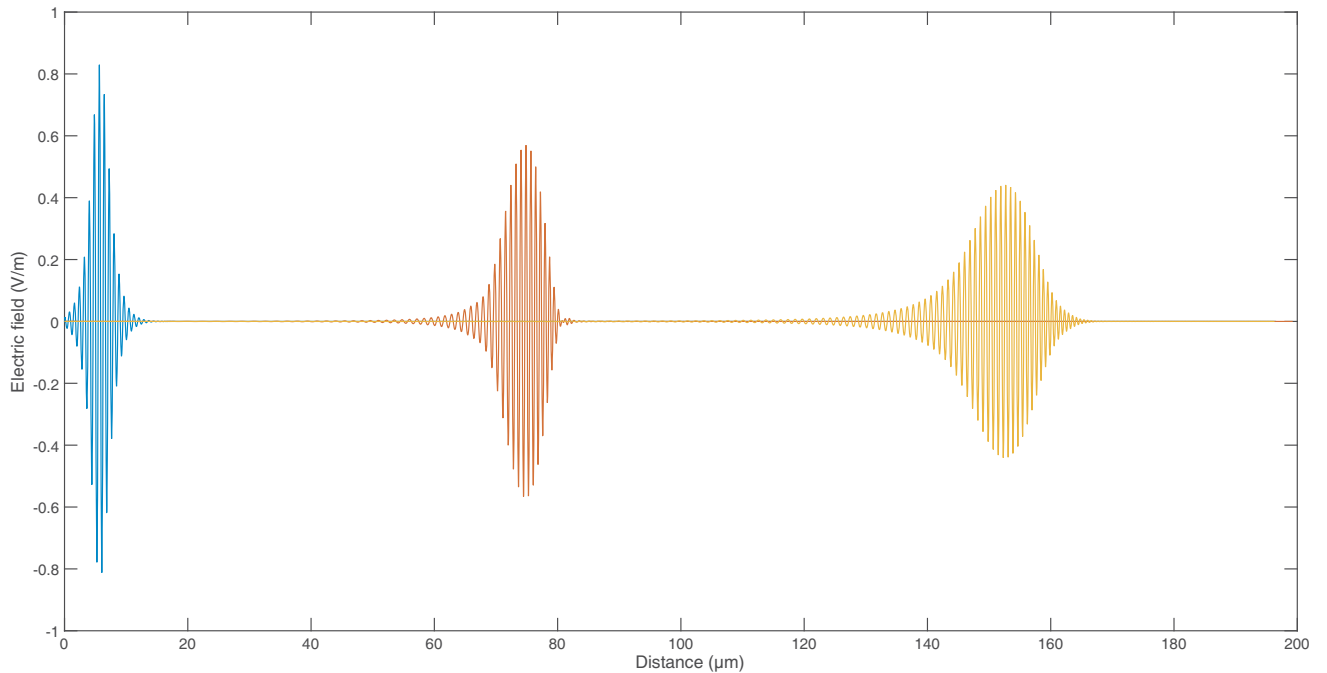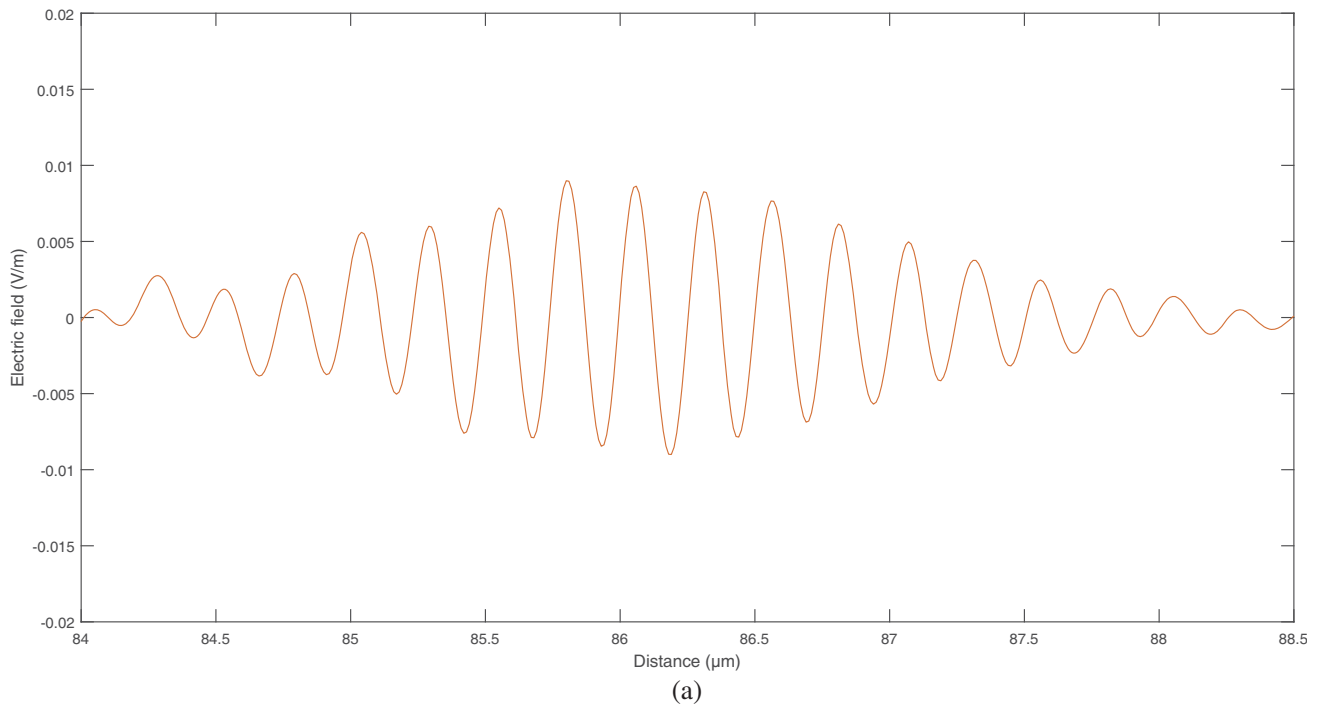

Figure 1. JE-TLM simulation results of the short pulse propagation in the Lorentz medium after 8000, 29000 and 56000 iterations.

For the Lorentz medium $w_L = 4 \times 10^{14} \, \text{rad/s}$, $\varepsilon_s = 5.25$, $\varepsilon_\infty = 2.25$ and $\delta_{Lorentz} = 2 \times 10^9 s^{-1}$. For the nonlinear Kerr and Raman media $\chi_0^{(3)} = 7 \times 10^{-2} (\text{V/m})^{-2}$, $\tau_1 = 12.2 \, \text{fs}$, $\tau_2 = 32 \, \text{fs}$ and $\alpha = 0.7$.

Figure 1, linear case $[\chi_0^{(3)} = 0]$, shows simulation result of pulse propagating after $6 \, \mu\text{m}$, $75 \, \mu\text{m}$ and $150 \, \mu\text{m}$ corresponding to propagation respectively to 8000, 29000 and 56000 iterations. The appearance of attenuation, broadening and modulation of the pulse carrier frequency is predicted as reported and presented in [10] and [14].
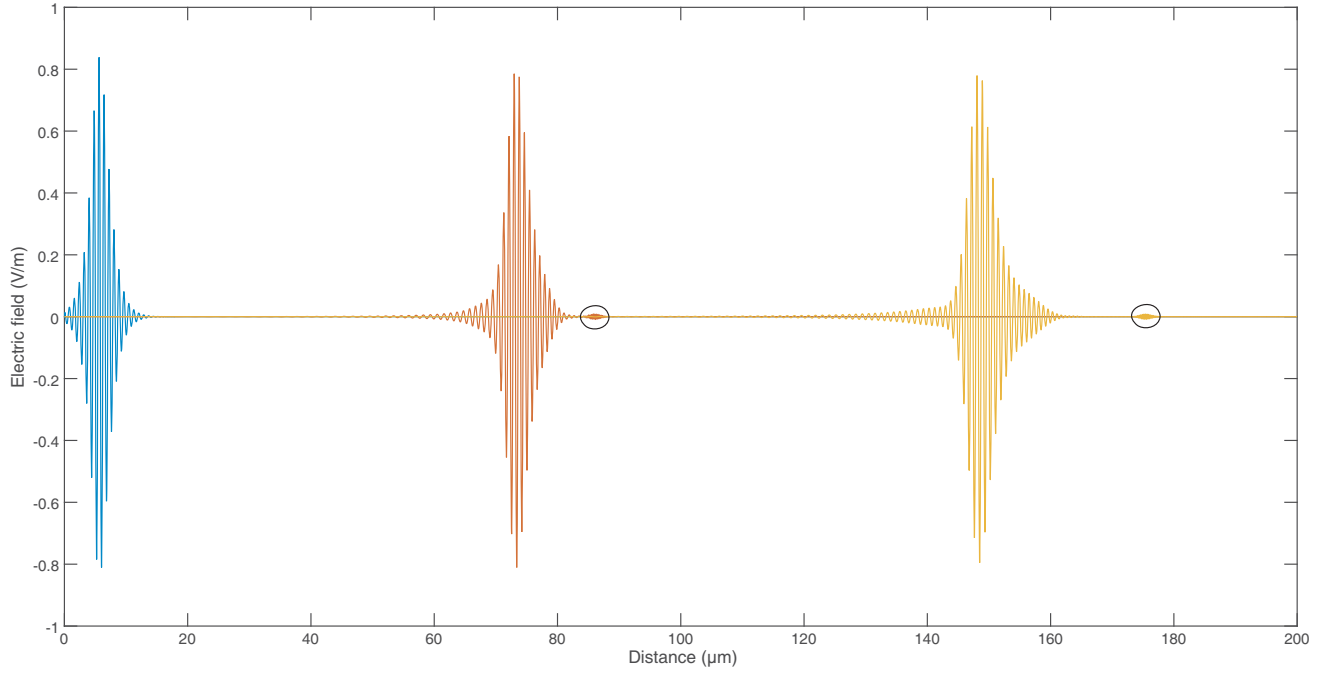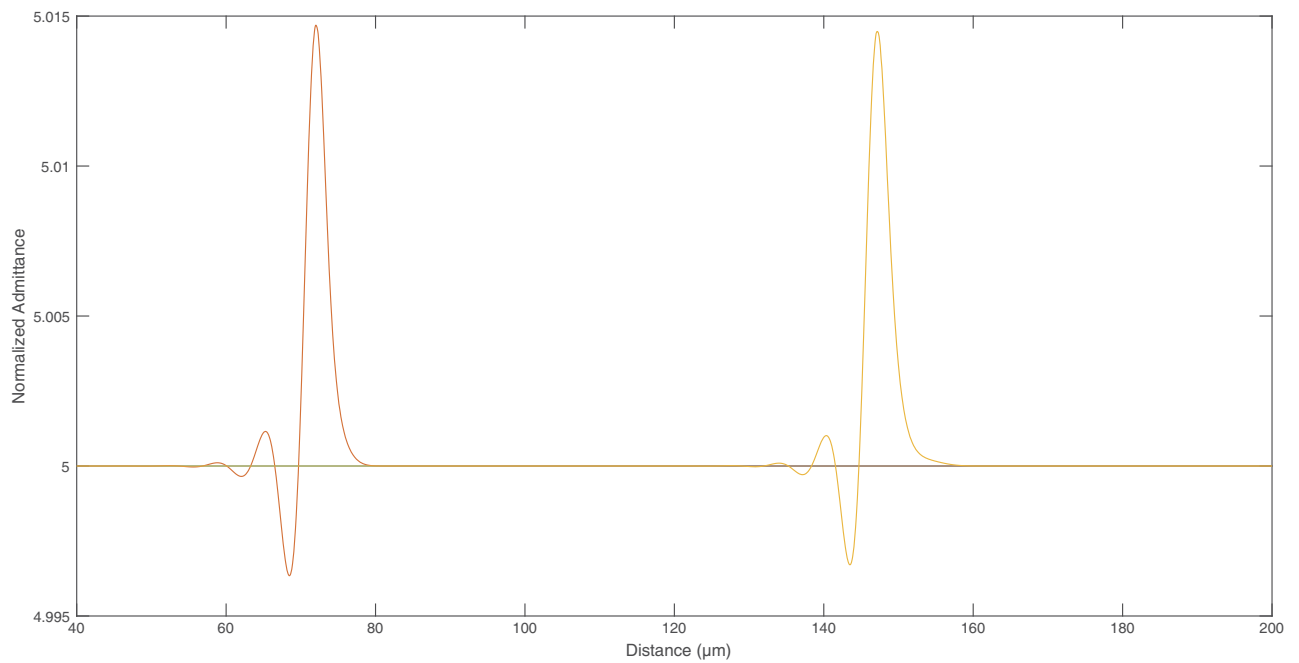

Figure 2. JE-TLM simulation results of the soliton propagation in the Kerr and the Raman medium after 8000, 29000 and 56000 iterations.

(a)

(b)
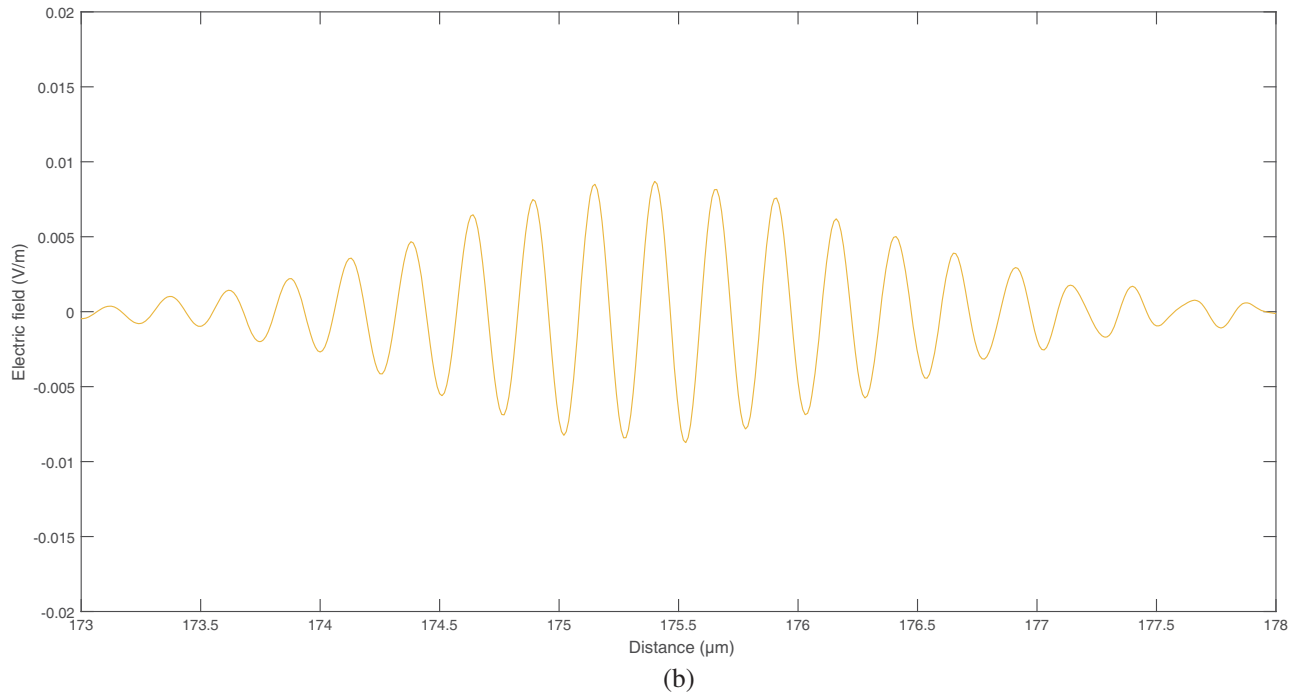
Figure 3. JE-TLM simulation results of small daughters pulses. (a) First daughter soliton. (b) Second daughter soliton.

Figure 4. JE-TLM simulation results of Normalized Admittance after 29000 and 56000 iterations.

Figure 2, nonlinear case $[\chi_0^{(3)} = 7 \times 10^{-2}(\mathrm{V/m})^{-2}]$, depicts the TLM simulation results that show the formation of a temporal soliton conserving its amplitude and width even at the distance of $150\,\mu\mathrm{m}$, followed by a small low-amplitude soliton (Figure 3). Those results are similar to those presented in [10] and [14].

Figure 4 shows the variation of the normalized nonlinear admittance propagating after 75 µm and 150 µm corresponding to propagation respectively to 29000 and 56000 iterations.

4. CONCLUSION

We have efficiently analyzed Maxwell's equations and different polarization expressions for spatio-temporal modeling propagation of optical pulses in linear and nonlinear dispersive media using the JE-TLM model. In this model, we introduce voltage sources modeling linear and nonlinear properties and variable admittance concept. The advantage of this new model is its modularity since it allows separately calculating each dispersion, and its accuracy is tested by the obtained numerical results. The good agreement between the novel JE-TLM approach results and those available in the literature proves its validity and efficiency.

REFERENCES

1. Franken, P. A., A. E. Hill, C. W. Peters, and G. Weinreich, "Generation of optical harmonics," *Phys. Rev. Lett.*, Vol. 7, No. 4, 118–119, 1961,

2. Agrawal, G. P., *Nonlinear Fiber Optics*, 4th Edition, Academic Press, New York, 2007.

3. Hasegawa, A. and F. Tappert, "Transmission of stationary nonlinear optical pulses in dispersive dielectric fibers: I. Anomalous dispersion," *Appl. Phys. Lett.*, Vol. 23, No. 3, 142–144, 1973.

4. Tran, P., "A nonlinear photonic crystal: A numerical study," *Optics Letters*, Vol. 21, No. 15, 1138–1140, 1996.

5. Cherenkov, A. V., N. M. Kondratiev, V. E. Lobanov, A. E. Shitikov, D. V. Skryabin, and M. L. Gorodetsk, "Raman-Kerr frequency combs in microresonators with normal dispersion," *Optics Express*, Vol. 25, No. 25, 31148–31158, 2017.

6. Fanjoux, G., A. Sudirman, J.-C. Beugnot, L. Furfaro, W. Margulis, and T. Sylvestre, "Stimulated Raman-Kerr scattering in an integrated nonlinear optofluidic fiber arrangement," *Optics Letters*, Vol. 39, No. 18, 5407-5407, 2014.

7. Karras, C., W. Paa, D. Litzkendorf, S. Grimm, K. Schuster, and H. Stafast, "SiO$_2$-Al$_2$O$_3$-La$_2$O$_3$ glass — A superior medium for optical Kerr gating at moderate pump intensity," *Optical Materials Express*, Vol. 6, No. 1, 125–130, 2016.

8. Garmire, E., "Nonlinear optics in daily life," *Optics Express*, Vol. 21, No. 25, 30532–30544, 2013.

9. Nakamura, S., N. Takasawa, and Y. Koyamada, "Comparison between finite-difference time-domain calculation with all parameters of Sellmeier's fitting equation and experimental results for slightly chirped 12 fs laser pulse propagation in a silica fiber," *IEEE J. of Lightwave Technol.*, Vol. 23, No. 2, 855–863, 2005.

10. Fujii, M., M. Tahara, I. Sakagami, W. Freude, and P. Russer, "High order FDTD and auxiliary differential equation formulation of optical pulse propagation in 2-D Kerr and Raman nonlinear dispersive media," *IEEE J. Quantum Electron.*, Vol. 40, No. 2, 175–182, 2004,

11. Johns, P. B., "A symmetrical condensed node for the TLM method," *IEEE Trans. Microwave Theory and Techniques*, Vol. 35, 370–377, 1987.

12. Paul, J., C. Christopoulos, and D. W. P. Thomas, "Generalized material models in TLM. I.: Materials with frequency-dependent properties," *IEEE Trans. Antennas Propag.*, Vol. 47, 1528–1534, 1999.

13. Yaich, M. I. and M. Khalladi, "A novel SCN-TLM model for the analysis of ferrite media," *IEEE Micro. Wireless Compn. Lett.*, Vol. 13, No. 6, 217–219, 2003.

14. El Faylali, H., "Modeling of optical pulse propagation in Kerr and Raman nonlinear dispersive media using ADE-TLM method," *International Journal of Advanced Engineering Technology*, Vol. IV, No. II, 1064–1076, 2013.

15. Abrini, R., M. Ibn Yaich, and M. Khalladi, "Efficient modeling of isotropic cold plasma media using JE-TLM method," *IEICE Electronics Express*, Vol. 4, No. 15, 492–497, 2007.

16. Charif, M., et al., "Accuracy and CPU time of JE-TLM, PLRC-TLM and CRC-TLM methods for plasma medium," *Optik — Int. J. Light Electron. Op.*, Vol. 125, No. 13, 3138–3141, 2014.

17. El Faylali, H., M. Iben Yaich, and M. Khalladi, "Modeling of optical pulse propagation in nonlinear dispersive media using JE-TLM method," *International Journal of Engineering Sciences & Research Technology*, Vol. 2, No. 5, 1308–1312, 2013.

18. Taflove, A. and S. C. Hagness, *Computational Electrodynamics: The Finite-Time Domain-Method*, Artech House, Norwood, MA, 1995.

19. Greene, J. H. and A. Taflove, "General vector auxiliary differential equation finite-difference time-domain method for nonlinear optics," *Journal Title Abbreviation*, Vol. 14, No. 18, 1064–1076, 2006.

20. Khalladi, M., M. I. Yaich, N. Aknin, and M. Carrion, "Modeling of electromagnetic waves propagation in nonlinear optical media using HSCN-TLM method," *IEICE Electronics Express*, Vol. 2, No. 13, 384–391, 2005.